

Spectroelectrochemical Evidence for the Nitrosyl Redox Siblings NO^+ , NO^\bullet , and NO^- Coordinated to a Strongly Electron-Accepting Fe^{II} Porphyrin: DFT Calculations Suggest the Presence of High-Spin States after Reduction of the $\text{Fe}^{\text{II}}\text{--NO}^-$ Complex

Juan Pellegrino,^[a] Ralph Hübner,^[b] Fabio Doctorovich,^{*,[a]} and Wolfgang Kaim^{*,[b]}

Abstract: Experimental and computational results for the electron-deficient porphyrin complex $[\text{Fe}(\text{NO})(\text{TFP-PBr}_8)]$ (**1**; $\text{TFPPBr}_8 = 2,3,7,8,12,13,17,18\text{-octabromo-5,10,15,20-tetrakis(pentafluorophenyl)-porphyrin}$) are reported with respect to its electron-transfer behavior. Complex **1** undergoes three one-electron processes: two reversible reductions and one irreversible oxidation. Spectroelectrochemical measurements (IR and UV/Vis/NIR spectroscopy) of ^{14}NO - and ^{15}NO -containing material indicate that the first reduction to $\mathbf{1}^-$ occurs

largely on the NO ligand to produce nitroxyl anion (NO^-) character, as evident from the considerable change in ν_{NO} from 1715 to around 1550 cm^{-1} . The second reduction to $\mathbf{1}^{2-}$ does not result in a further shift of ν_{NO} to lower frequencies, but to a surprising high-energy shift to 1590 cm^{-1} . This and the notable changes of the characteristic porphyrin vibrations as well as signifi-

cant changes of the UV/Vis absorptions indicate a porphyrin-centered process; DFT calculations predict the shift of ν_{NO} to higher frequencies for the intermediate- and high-spin states of $\mathbf{1}^{2-}$. The oxidation of **1** is irreversible on the voltammetry timescale, but chemically reversible in spectroelectrochemical experiments, suggesting that the cationic form dissociates to the corresponding ferric porphyrin and NO. DFT calculations support the interpretation of the experimental results.

Keywords: density functional calculations • iron • nitric oxide • porphyrins • spectroelectrochemistry

Introduction

Coordination compounds of the type $\{\text{MNO}\}^{n[1]}$ have experienced renewed attention since the discovery of the nitric oxide radical NO^\bullet as a physiologically essential agent. In 1992, NO was therefore voted the molecule of the year by the journal *Science*.^[2] Many processes of NO formation, release, and binding involve metal–NO interactions.^[3] More

specifically, there is growing interest in the chemistry of heme–nitrosyl systems because both the formation and activity of NO in vivo are mediated by heme proteins.^[4] Due to the general importance of the heme–NO interaction, a large amount of research has been devoted to the synthesis of corresponding model systems. These investigations employed synthetic porphyrins such as tetraphenylporphyrin (TPP) or the more electron-rich octaethylporphyrin (OEP), and iron nitrosyl complexes of these standard porphyrins have been extensively studied.^[5] Ruthenium nitrosyl porphyrins have also been used as heme models because of their enhanced stability relative to iron nitrosyl complexes.^[6] In addition to $\{\text{FeNO}\}^7$ porphyrin complexes, the one-electron oxidized and reduced forms $\{\text{FeNO}\}^6$ and $\{\text{FeNO}\}^8$, respectively, have been proposed as biorelevant species.^[7] A better understanding of the structure and reactivity of those complexes is desirable and could help to elucidate mechanistic issues. Therefore, several studies on the electron-transfer behavior of $\{\text{MNO}\}^n$ complexes have been reported.^[8]

In the case of $\{\text{FeNO}\}^n$ porphyrinato complexes, the $\{\text{FeNO}\}^7$ systems were by far the most extensively studied.^[9] It has been established that the related $\{\text{FeNO}\}^{6/8}$ complexes are more reactive and readily lose the NO ligand or convert to the $\{\text{FeNO}\}^7$ form.^[9–11] The pioneering reports by Kadish et al. on the spectroelectrochemical oxidation and reduction of the $\{\text{FeNO}\}^7(\text{Porph})$ (Porph = porphyrinato ligand) complexes $[\text{Fe}(\text{NO})(\text{TPP})]$ and $[\text{Fe}(\text{NO})(\text{OEP})]$ provided the

[a] J. Pellegrino, Prof. Dr. F. Doctorovich
Departamento de Química Inorgánica, Analítica, y Química Física
Facultad de Ciencias Exactas y Naturales
Universidad de Buenos Aires. INQUIMAE-CONICET
Ciudad Universitaria, Pab. 2
C1428EHA Buenos Aires (Argentina)
Fax: +54 11 4576-3341
E-mail: doctorovich@qi.fcen.uba.ar

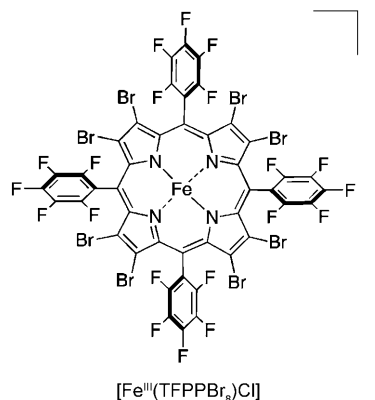
[b] Dipl.-Chem. R. Hübner, Prof. Dr. W. Kaim
Institut für Anorganische Chemie
Universität Stuttgart
Pfaffenwaldring 55
70550 Stuttgart (Germany)
Fax: (+49) 711 685 64165
E-mail: kaim@iac.uni-stuttgart.de

Supporting information for this article is available on the WWW under <http://dx.doi.org/10.1002/chem.201003516>. It contains observed UV/Vis spectral changes during the first electrochemical reduction of **1**; EPR of **1**; UV/Vis spectra data for **1**, $\mathbf{1}^-$, and $\mathbf{1}^{2-}$; and cartesian coordinates from optimizations of $\mathbf{1}^{2-}$ and $\mathbf{1}^+$.

first evidence of $\{\text{FeNO}\}^{6/8}(\text{Porph})$ species, in dichloromethane.^[11] In a subsequent paper, electrochemical measurements of different $\{\text{FeNO}\}^7(\text{Porph})$ compounds (Porph = porphyrins, hydroporphyrins, and porphines) allowed the site of electron transfer for two oxidation and two reduction steps to be determined: the first reduction and the second oxidation were proposed to be centered on the $\text{Fe}(\text{NO})$ moiety, thus yielding $[\{\text{FeNO}\}^8(\text{Porph}^{2-})]^-$ and $[\{\text{FeNO}\}^6(\text{Porph}^-)]^{2+}$ species, respectively, while the first oxidation and the second reduction would lead to the formation of porphyrin π radicals.^[12] More recently, FTIR spectroelectrochemical measurements and computational studies were conducted for some of the $[\text{Fe}(\text{NO})(\text{Porph})]$ compounds previously studied; these studies confirmed that the first reduction was highly NO centered.^[13] However, the second reduction was not studied, probably due to the high reactivity of the $[\text{Fe}(\text{NO})(\text{Porph})]^{2-}$ products. There have also been studies on the spectroelectrochemistry of cobalt nitrosyl porphyrins in which the site of the redox process was envisioned on the basis of the shift of $E_{1/2}$ potentials by ring substitution and through the observed UV/Vis and IR spectral changes relative to previously reported similar systems.^[14] These studies have also been expanded to manganese, ruthenium, and osmium nitrosyl porphyrinato complexes.^[8e,f,h] For these complexes, all three components—the porphyrinato ligands, the metal, and NO—are redox active in the central redox potential region, so that the determination of individual oxidation-state combinations is not trivial. In recent contributions, the combination of experimental results with DFT calculations is a powerful method to unambiguously

determine the site of the redox processes in such complex systems.^[8,13]

In a recent paper,^[15] we reported that $[\text{Fe}^{\text{III}}(\text{TFPPBr}_8)\text{Cl}]$ ($\text{TFPPBr}_8 = 2,3,7,8,12,13,17,18$ -octabromo-5,10,15,20-tetrakis(pentafluorophenyl)porphyrin), containing strongly accept-



ing substituents, can form the $\{\text{FeNO}\}^7$ nitrosyl iron complex $[\text{Fe}(\text{NO})(\text{TFPPBr}_8)]$ (**1**), which undergoes two reversible one-electron reduction processes and one irreversible oxidation in CH_2Cl_2 . Focusing on the stabilization of the heme model $\{\text{FeNO}\}^8$ moiety, we reported the preparation and spectroscopic characterization of the complex $[\text{Co}(\text{C}_5\text{H}_5)_2]^+ \mathbf{1}^-$, obtained from one-electron chemical reduction of **1**. Both experimental and computational data allowed us to assign the electronic structure of $[\text{Co}(\text{C}_5\text{H}_5)_2]^+ \mathbf{1}^-$ as intermediate between $\text{Fe}^{\text{II}}(\text{NO}^-)$ and $\text{Fe}^{\text{I}}(\text{NO}^*)$, which contrasted with the predominant $\text{Fe}^{\text{II}}(\text{NO}^-)$ character of known non-heme $\{\text{FeNO}\}^8$ complexes.^[8a] Following that study, we now report experimental (UV/Vis and IR spectroelectrochemical) and computational results for all three electron-transfer processes of **1**. Thus, we complete the characterization of $\mathbf{1}^-$, and we now focus on the other electron-transfer products of **1**, the potential $\{\text{FeNO}\}^9$ state in $\mathbf{1}^{2-}$ —possibly involving the NO^{2-} radical—and on the $\{\text{FeNO}\}^6$ complex, $\mathbf{1}^+$. The experimental results are interpreted through DFT calculations.

Results and Discussion

Cyclic voltammetry: Figure 1 shows a typical cyclic voltammogram of **1** in CH_2Cl_2 . Three single-electron-transfer processes are observed within the solvent window, which can be represented by Equations (1)–(3).



Abstract in Spanish: En este trabajo se estudia el comportamiento redox del complejo $[\text{FeNO}]^7$ con sustituyentes atractores de electrones, $[\text{Fe}(\text{NO})(\text{TFPPBr}_8)] = \mathbf{1}$ ($\text{TFPPBr}_8 = 2,3,7,8,12,13,17,18$ -octabromo-5,10,15,20-tetrakis(pentafluorofenil)porfirina) mediante experimentos de espectroelectroquímica y cálculos computacionales. El complejo **1** presenta tres procesos electroquímicos de un electrón: dos reducciones reversibles y una oxidación irreversible. El considerable cambio de ν_{NO} de 1715 cm^{-1} a $\approx 1550 \text{ cm}^{-1}$ indica que la primera reducción a $\mathbf{1}^-$ involucra en gran medida al ligando NO. Para la segunda reducción a $\mathbf{1}^{2-}$ se observa, sorprendentemente, un cambio de ν_{NO} a $\approx 1590 \text{ cm}^{-1}$. Este pequeño corrimiento de ν_{NO} y los cambios notables de las vibraciones asociadas a modos de la porfirina, así como los cambios significativos en la banda UV/Vis de Soret, indican un proceso centrado en la porfirina; los cálculos DFT predicen el corrimiento de ν_{NO} a mayores frecuencias para los estados de spin intermedio y alto de $\mathbf{1}^{2-}$. En cuanto a la oxidación de **1**, la onda irreversible en la voltametría cíclica sugiere que la forma catiónica $\mathbf{1}^+$ se disocia dando la porfirina de hierro(III) y NO; sin embargo, en el experimento espectroelectroquímico el proceso resulta reversible, recuperándose la ν_{NO} de **1** al reducir. Los cálculos DFT apoyan la interpretación de los resultados experimentales.

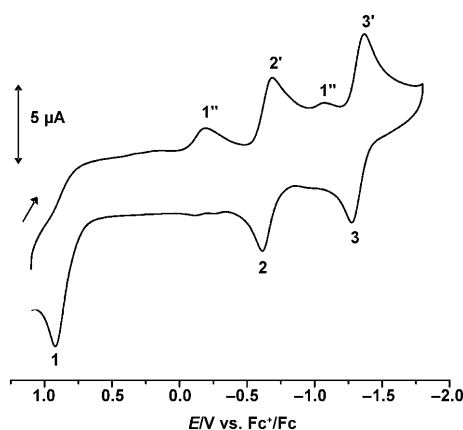
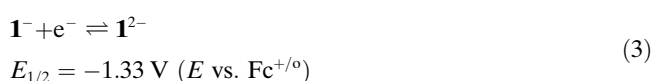


Figure 1. Cyclic voltammogram of **1** in CH₂Cl₂/0.1 M Bu₄NPF₆ at 100 mV s⁻¹.



The couples 2-2' and 3-3' (Figure 1) represent the two reversible reductions of **1** [Eqs. (2) and (3)] that are shifted +770 and +940 mV from the corresponding values of the analogous complex without the halogen substituents, [Fe(NO)(TPP)] (**2**).^[11,16] Complex **2** exhibits three oxidation waves within the solvent window, while **1** exhibits only one chemically irreversible oxidation at $E_{pa} = +0.92$ V (labeled 1 in Figure 1), shifted by +670 mV relative to the first oxidation step of **2**. This irreversible oxidation process is associated with two small return reduction features at about -0.2 and -1.1 V (1'' in Figure 1), which correspond to the couples Fe^{III}(TFPPBr₈)⁺/Fe^{II}(TFPPBr₈) and Fe^{II}(TFPPBr₈)/Fe^I(TFPPBr₈)⁻, respectively.^[17] These signals are absent in the voltammogram when the oxidation potential is not reached, confirming that they correspond to a species generated after the oxidation of **1**. This result suggests that the NO ligand is lost once the oxidized species **1**⁺ is formed, as shown in Equation (4):



As stated in the Introduction, there are previous reports on the lability of the NO ligand in {FeNO}⁶ porphyrin complexes,^[9] and a recent theoretical study showed that this instability is associated with the presence of high-spin states lying close to the low-spin ground state.^[10]

Spectroelectrochemistry: The reversibility of the first and second reduction waves allowed us to characterize the reduction products of **1**, **1**⁻, and **1**²⁻ through spectroelectrochemical methods. Both in the UV/Vis and IR absorption experiments, the reductions were fully reversible and we could recover the spectrum of **1** upon reoxidation. Figure S1 in the Supporting Information and Figure 2 show the UV/Vis and IR spectra, respectively, obtained on electrochemical reduction of **1** to **1**⁻.

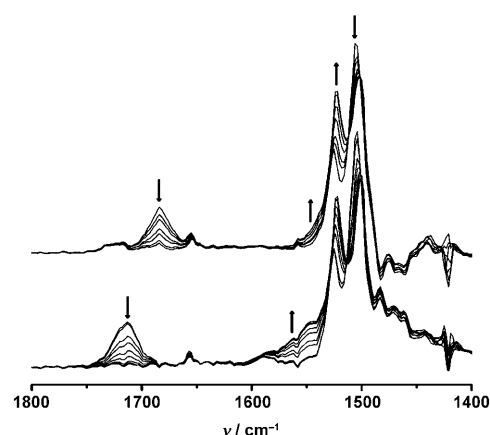


Figure 2. IR spectral changes observed during the electrochemical reduction of **1** (bottom) and ¹⁵N-labeled **1** (top) in CH₂Cl₂/0.1 M Bu₄NPF₆.

The minor changes in the Soret band of the UV/Vis spectrum upon one-electron reduction were similarly to those observed previously;^[11,16] they suggest a non-porphyrin-based reduction. Moreover, the significant change of $\Delta\nu \approx -165$ cm⁻¹ observed in the IR spectrum for the NO stretching frequency—from 1715 to about 1550 cm⁻¹—is indicative of a largely NO-centered reduction. Thus, the first reduction product of **1** can be described as [FeNO]⁸(TFPPBr₈)²⁻, as has been suggested before.^[15] The NO stretching band assignment was confirmed by an experiment with ¹⁵N-labeled **1**, [Fe^{II}(¹⁵NO)(TFPPBr₈)]. We found the expected shift to lower frequencies in the NO stretching features; unfortunately, the NO stretching band of the reduced labeled product **1**⁻ was obscured by intense porphyrin vibrational bands at around 1500–1550 cm⁻¹. The changes observed on electrochemical reduction of **1** to **1**⁻ are consistent with those found after the chemical reduction of **1** with cobaltocene, yielding [Co(C₅H₅)₂]⁺**1**⁻.^[15] Moreover, we monitored the electrochemical reduction of **1** by EPR spectroscopy and found the intensity of the radical signal decreased while no other signal appeared. Figure S2 in the Supporting Information shows a typical EPR spectrum of **1**. This result is consistent with the expected diamagnetic product **1**⁻.

Since there is a second, reversible reduction wave in the cyclic voltammogram of **1**, we also set out to characterize the second reduction product of **1**, **1**²⁻ [Eq. (3)], which could give rise to an {FeNO}⁹ complex containing the NO²⁻ ion.^[18] Figure 3 shows the UV/Vis and IR spectra obtained on electrochemical reduction of **1**⁻ to **1**²⁻. In both the UV/Vis and IR experiments, the reduction was fully reversible and we could recover the spectrum of **1**⁻ on reoxidation, indicating that **1**²⁻ is a relatively stable product.

Significant changes in the Soret and Q bands were noted previously after reduction of **2**⁻;^[11,16] this indicated a porphyrin-centered process and vibrational spectra could not be obtained. The changes of the IR bands in the present case with shifts from 1522 and 1500 to 1516 and 1494 cm⁻¹, respectively, suggest a reduction of the porphyrin ring. The NO stretching band was observed to shift from 1550 cm⁻¹ to

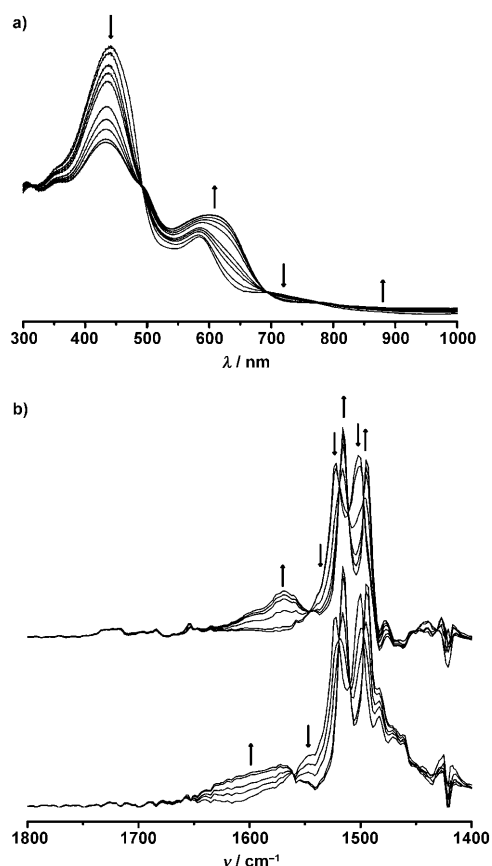


Figure 3. a) UV/Vis spectral changes observed during the electrochemical reduction of **1**⁻ to **1**²⁻ in CH₂Cl₂/0.1 M Bu₄NPF₆. b) IR spectral changes observed during the electrochemical reduction of **1**⁻ (bottom) and of ¹⁵N labeled **1**⁻ (top) in CH₂Cl₂/0.1 M Bu₄NPF₆.

yield a broad asymmetric band around 1590 cm⁻¹. If the second reduction product, **1**²⁻, corresponds to a nitroxyl ferrous porphyrin radical complex, [(FeNO)⁸(TFPPBr₈³⁻)]²⁻, this should result in an EPR signal at *g* ≈ 2.00 and produce a slightly lowered value of *ν*_{NO} (see the DFT calculations section). However, no EPR signal was observed at *g* ≈ 2.00 at room temperature or at 243 K. On the other hand, *ν*_{NO} shifts to higher values, and the DFT calculations (see below) suggest alternative descriptions, such as [(FeNO)⁷(TFPPBr₈⁴⁻)]²⁻, with higher spin states to account for the experimental results.

The irreversibility of the oxidation in the cyclic voltammogram of **1** (Figure 1) prompted us to confirm that the suspected reaction [Eq. (4)] is taking place after the initial electron transfer.

After oxidation of **1**, a new broad signal at around 1830 cm⁻¹ appears in the IR spectrum, while the *ν*_{NO} feature of **1** at 1716 cm⁻¹ disappears (Figure 4). The new signal is close to the stretching frequency of free NO (*ν*_{NO} = 1840 cm⁻¹).^[7] In the experiment with ¹⁵N-labeled **1**, this signal is shifted by -30 cm⁻¹ as expected. In spite of the observed irreversibility of the oxidation wave in the cyclic voltammetry experiment, we could recover the spectrum of **1** on re-reduction. A possible explanation for this reversibility

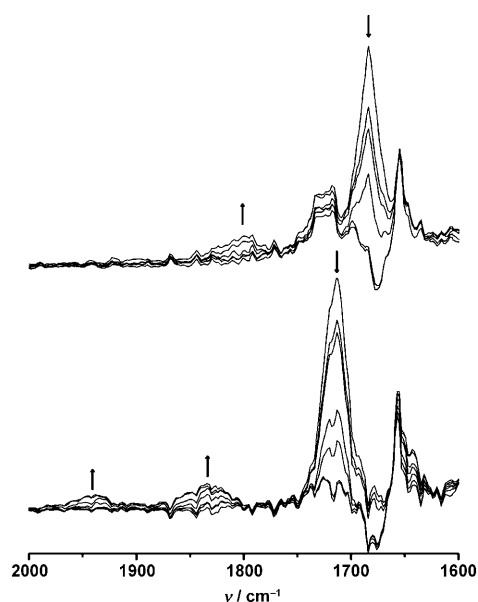
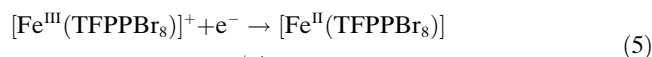


Figure 4. IR spectral changes observed during the electrochemical oxidation of **1** (bottom) and ¹⁵N labeled **1** (top) in CH₂Cl₂/0.1 M Bu₄NPF₆.

in the spectroelectrochemical experiment is that the ferric porphyrin [Fe^{III}(TFPPBr₈)]⁺ is reduced to the ferrous state, [Fe^{II}(TFPPBr₈)], and then reacts with NO present in solution to give back **1** [Eqs. (5) and (6)].



$$E_{1/2} = -0.20 \text{ V vs. Fc}^+/\text{Fc}$$



Figure 4 reveals that a new broad band appears around 1930 cm⁻¹, in the range expected for the *ν*_{NO} of a {FeNO}⁶ porphyrin complex.^[9] This suggests that **1**⁺ is in equilibrium with the ferric porphyrin and NO, according to Equation (4). The +215 cm⁻¹ shift in *ν*_{NO} on conversion of **1** to **1**⁺ is indicative of a largely NO-centered oxidation, so that the electronic structure of **1**⁺ is described as [{FeNO]⁶(TFPPBr₈²⁻)]⁺, which is also in agreement with the following DFT calculations.

DFT calculations: DFT calculations were performed to obtain more insight into the electronic structures of the complexes and to support the interpretation of the IR spectral changes observed for the three electron-transfer processes.

Table 1 shows the relevant bond distances and angles for the calculated structures of **1** (*S* = 1/2), **1**⁻ (*S* = 0 and 1), **1**²⁻ (*S* = 1/2, 3/2, and 5/2), and **1**⁺ (*S* = 0).

The bonding parameters calculated for **1** and **1**⁻ are in good agreement with those found for related complexes, as discussed in a recent report.^[15] The calculations also illustrate the parameter changes observed when going from {FeNO}⁷ to {FeNO}⁶ (**1** → **1**⁺), that is, the shortening of the N–O and Fe–N(O) distances and the increase of the FeNO

Table 1. Selected bond lengths [Å] and angles [°] for calculated structures of **1**, **1⁻**, **1²⁻**, and **1⁺**.

	<i>d</i> (NO)	<i>d</i> (FeN)	∠FeNO	Ref.
1 (<i>S</i> = 1/2)	1.182	1.711	144.4	[15]
1⁻ (<i>S</i> = 0)	1.201	1.790	122.7	[15]
1⁻ (<i>S</i> = 1)	1.181	1.747	154.8	[15]
1²⁻ (<i>S</i> = 1/2)	1.204	1.756	128.4	this work
1²⁻ (<i>S</i> = 3/2)	1.193	1.699	143.9	this work
1²⁻ (<i>S</i> = 5/2)	1.186	1.742	152.9	this work
1⁺ (<i>S</i> = 0)	1.166	1.623	180.0	this work

angle from a bent to a linear structure.^[9] Most intriguingly, the parameters related to the FeNO moiety for **1²⁻** are very dependent on the spin state. The parameters for the intermediate- and high-spin states are remarkably different from the ones for the low-spin state, for example, the FeNO angle changes from 128.4 to 152.9°. These results can be rationalized by assuming an electronic redistribution for the higher spin states of **1²⁻**, yielding an electronic structure best described as $[(\text{FeNO})^7(\text{TFPPBr}_8^{4-})]^{2-}$ instead of the $[(\text{FeNO})^8(\text{TFPPBr}_8^{3-})]^{2-}$ description befitting the low-spin state. As reported previously,^[15] a similar change in the electronic structure was observed for the singlet and triplet states of **1⁻**. While the singlet state is best described as $[(\text{FeNO})^8(\text{TFPPBr}_8^{2-})]^-$, the triplet state can be rationalized as $[(\text{FeNO})^7(\text{TFPPBr}_8^{3-})]^-$. This dependence of the electronic structure on the spin state has been observed and discussed before for $[\text{Fe}(\text{MI})(\text{NO})(\text{porphine})]^-$ (MI = 1-methylimidazole, porphine = unsubstituted porphyrin).^[19] In addition, a normal population analysis (NPA) was done to investigate the charge distribution for the complexes **1²⁻** in the three different spin states (Table 2). Both the intermediate- and

Table 2. Relative energies and calculated natural population analysis (NPA) for **1^{2-<M>}** in three different spin states.

	Energy [kcal mol ⁻¹]	Fe	Charge NO	Porph
1²⁻ (<i>S</i> = 1/2)	0	0.58	-0.18	-2.40
1²⁻ (<i>S</i> = 3/2)	+2.7	0.68	-0.08	-2.60
1²⁻ (<i>S</i> = 5/2)	+15.3	1.16	-0.15	-3.01

high-spin states show a more negatively charged porphyrin ligand and consequently a less-electron-rich FeNO moiety compared with the low-spin state. This is consistent with the proposed change in the electronic structure, as discussed above. The DFT results suggest that the *S* = 3/2 state lies only 2.7 kcal mol⁻¹ above the low-spin state, which agrees with an important contribution of this state to the ground state of **1²⁻**. Moreover, most commonly used DFT functionals tend to favor low-spin transition-metal spin states;^[20] the relative stabilization of the intermediate-spin state may thus even be underestimated.

To determine the effect of the withdrawing groups on the electronic structure of **1²⁻**, we performed similar calculations on $[\text{Fe}(\text{NO})(\text{porphine})]^{2-}$. We found similar results regard-

ing the electronic redistribution for the intermediate- and high-spin states, but in this case, the relative energies of these states were higher, amounting to 7.4 and 19.6 kcal mol⁻¹ for the intermediate- and high-spin forms, respectively. Thus, the calculations confirm that the electron-withdrawing groups in **1²⁻** contribute to the stabilization of higher-spin states, which could also be related to the saddle distortion produced by the substituents. The existence of intermediate-spin states for saddle-distorted iron porphyrins has been reported.^[21]

IR frequencies for **1** in different oxidation and spin states were calculated to further support the spectroelectrochemical results (Table 3).

Table 3. Experimental and calculated ν_{NO} bands for **1**, **1⁻**, **1²⁻** and **1⁺**.

	Experimental [cm ⁻¹]	Calculated [cm ⁻¹]
1	1715 ^[a]	1759
1⁻	1550 ^[b]	1635 ^[c]
1²⁻	1590 ^[a]	1609 (<i>S</i> = 1/2); 1716 (<i>S</i> = 3/2); 1758 (<i>S</i> = 5/2)
1⁺	1930 ^[a]	1918
1 → 1⁺	+215	+159
1 → 1⁻	-165	-124
1 → 1²⁻	+40	-26 (<i>S</i> = 1/2); +81 (<i>S</i> = 3/2); +123 (<i>S</i> = 5/2)

[a] From spectroelectrochemical experiments in CH₂Cl₂. [b] From solid-state spectra of chemically prepared **1⁻**.^[15] [c] Strongly mixed with *meso*-phenyl modes.

In agreement with the spectroelectrochemical results, the calculations predict a significant shift of ν_{NO} for the first reduction and for the first oxidation, supporting the electronic structures assigned above. The best descriptions for the electronic structures of **1⁺**, **1**, and **1⁻** are still $[(\text{FeNO})^6(\text{TFPPBr}_8^{2-})]^+$, $[(\text{FeNO})^7(\text{TFPPBr}_8^{2-})]^0$, and $[(\text{FeNO})^8(\text{TFPPBr}_8^{2-})]^-$, respectively; thus, in the two processes, the FeNO moiety is essentially the site of electron transfer. However, if we compare the ν_{NO} values with those from complexes of other porphyrins without electron-withdrawing groups (e.g., TPP or OEP), they are shifted to higher frequencies for the three states; this can be explained by assuming less donation from the metal center to the NO ligand.^[4a] For the second reduction, the shift to higher frequencies observed in the experiment is only predicted for the intermediate- and high-spin states (Table 3). From the IR spectroelectrochemical results for the second reduction and the DFT calculations, the spin state *S* = 3/2 appears to be a valid description of the ground state of **1²⁻**. Accordingly, we propose one of the following three possibilities: 1) *S* = 3/2 is the ground state for **1²⁻**, 2) the ground state is a quantum-mechanical spin-state admixture with an important contribution of the *S* = 3/2 state, or 3) at least two spin states (*S* = 1/2, 3/2, and/or 5/2) are present in thermal equilibrium. The three situations are compatible with the experimental and computational results; the two last situations, although less common, are not unprecedented for iron porphyrins^[22] and

the very broad N–O stretching signal of $\mathbf{1}^{2-}$ suggests that the third situation could be taking place.

Conclusion

Spectroelectrochemical experiments and DFT calculations have allowed us to assign the electronic structures in the iron nitrosyl redox series $\mathbf{1}^{+/0/-/2-}$ of the strongly electron-accepting perhalogenated porphyrin TFPPBr₈. The strong electron-accepting propensity (ca. 0.8 V potential shift vs. TPP) facilitates the reduction of the corresponding neutral complex to the mono- and dianion, allowing the measurement of the vibrational spectrum of a $[\text{Fe}(\text{NO})(\text{Porph})]^{2-}$ species for the first time.

The reversible first reduction involves a large shift of $\nu(\text{NO})$ from 1715 to 1550 cm^{-1} , suggesting predominant NO reduction to $[\{\text{FeNO}\}^8(\text{TFPPBr}_8^{2-})]^-$. The oxidation also involves a large shift of $\nu(\text{NO})$ to 1930 cm^{-1} , suggesting predominant NO oxidation to $[\{\text{FeNO}\}^6(\text{TFPPBr}_8^{2-})]^+$, which is unstable towards dissociation of the NO ligand.

The reversible second reduction, starting from the $\text{Fe}^{\text{II}}(\text{NO}^-)$ porphyrin would be expected to produce a shift of $\nu(\text{NO})$ to lower frequencies due to NO^- or porphyrin-centered reduction. Surprisingly, this reduction is accompanied by a positive shift of $\nu(\text{NO})$ of 40 cm^{-1} , apart from notable changes in the porphyrin absorptions (UV/Vis, IR spectroscopy). It is therefore assumed that this is a porphyrin-based reduction that leads to a species best formulated as $[\{\text{FeNO}\}^7(\text{TFPPBr}_8^{4-})]^{2-}$ with a higher spin state. This electronic configuration would account for the positive shift of $\nu(\text{NO})$, as confirmed by DFT calculations for intermediate- and high-spin states. This electronic redistribution demonstrates the pronounced noninnocent ligand behavior of $(\text{TFPPBr}_8)^{n-}$.^[23]

Experimental Section

Syntheses: 5, 10, 15, 20-Tetrakis(pentafluorophenyl)porphyrin (H_2TFPP) was purchased from Frontier Scientific and used as received. All solvents were distilled and dried according to conventional procedures. The porphyrin ligand TFPPBr₈ and the iron(III) complex $\text{Fe}(\text{TFPPBr}_8)\text{Cl}$ were prepared according to slightly modified published procedures, starting from H_2TFPP , as described before.^[15,24]

$[\text{Fe}(\text{NO})(\text{TFPPBr}_8)]$ ($\mathbf{1}$): Complex $\mathbf{1}$ and the ^{15}N enriched compound were prepared as described before.^[15]

Physical measurements: Cyclic voltammetry was carried out at a scan rate of 100 mV s^{-1} in dry and deoxygenated $\text{CH}_2\text{Cl}_2/0.1\text{ M Bu}_4\text{NPF}_6$ using a three-electrode configuration (glassy carbon or Pt working electrode, Pt counter electrode, Ag wire pseudoreference electrode) and a PAR 273 potentiostat and function generator. The ferrocenium/ferrocene ($\text{Fc}^{+/0}$) couple served as an internal reference. The solutions were prepared under Ar or N_2 in a dry box or by using a vacuum line at concentrations of approximately 1 mM.

UV/Vis/NIR absorption spectra were recorded on a J&M TIDAS spectrophotometer. IR spectra were obtained by using a Nicolet 6700 FT-IR instrument. Spectroelectrochemistry was performed by using an OTTLE cell in dry and deoxygenated $\text{CH}_2\text{Cl}_2/0.1\text{ M Bu}_4\text{NPF}_6$.

Computational methodology: All calculations were carried out with the program package Gaussian 03.^[25] The structures of all molecules were fully geometry optimized at the DFT level, using the PBE exchange-correlation functional. The LANL2DZ basis set and pseudopotentials were used for the Fe atom. For the remaining atoms (H, N, O, C, F, and Br) the 6-31G** basis set was used. Charges were calculated by performing a natural population analysis (NPA). The vibrational frequencies were calculated on optimized structures by using the same functional and basis set.

Acknowledgements

This work was financially supported by the University of Buenos Aires (UBACYT X065), ANPCyT (PICT 2006–2396) and CONICET. Support by Deutsche Forschungsgemeinschaft and DAAD is also acknowledged. We thank Dr. Brigitte Schwederski for performing EPR measurements.

- [1] $\{\text{FeNO}\}^n$ is the generalized description of the metal–NO bonding, in which n is the sum of the metal d electrons and the nitrosyl π^* electrons, see: J. H. Enemark, R. D. Feltham, *Coord. Chem. Rev.* **1974**, *13*, 339–406.
- [2] D. E. Koshland, *Science* **1992**, *258*, 1861.
- [3] a) L. Cheng, G. B. Richter-Addo in *The Porphyrin Handbook*, Vol. 4 (Eds.: R. Guilard, K. Smith, K. M. Kadish), Academic Press, New York, **2000**, Chapter 33; b) P. C. Ford, L. E. Laverman, I. M. Lorkovic, *Adv. Inorg. Chem.* **2003**, *54*, 203–257; c) A. R. Butler, C. Glidewell, M.-H. Li, *Adv. Inorg. Chem.* **1988**, *32*, 335–393; d) C. Selcuki, R. van Eldik, T. Clark, *Inorg. Chem.* **2004**, *43*, 2828–2833, and references therein; e) V. S. Sharma, R. B. Pilz, G. R. Boss, D. Magde, *Biochemistry* **2003**, *42*, 8900–8908, and references therein.
- [4] a) L. E. Goodrich, F. Paulat, V. K. K. Praneeth, N. Lehnert, *Inorg. Chem.* **2010**, *49*, 6293–6316; b) D. D. Thomas, K. M. Miranda, C. A. Colton, D. Citrin, M. G. Espey, D. A. Wink, *Antioxid. Redox Signaling* **2003**, *5*, 307–317.
- [5] a) P. C. Ford, I. M. Lorkovic, *Chem. Rev.* **2002**, *102*, 993–1017; b) V. K. K. Praneeth, F. Neese, N. Lehnert, *Inorg. Chem.* **2005**, *44*, 2570–2572; c) G. R. A. Wyllie, C. E. Schulz, W. R. Scheidt, *Inorg. Chem.* **2003**, *42*, 5722–5734; d) V. K. K. Praneeth, C. Näther, G. Peters, N. Lehnert, *Inorg. Chem.* **2006**, *45*, 2795–2811; e) V. K. K. Praneeth, E. Haupt, N. Lehnert, *J. Inorg. Biochem.* **2005**, *99*, 940–948; f) I. V. Novozhilova, C. Philip, J. Lee, G. B. Richter-Addo, K. A. Bagley, *J. Am. Chem. Soc.* **2006**, *128*, 2093–2104; g) G. B. Richter-Addo, R. A. Wheeler, C. A. Hixson, L. Chen, M. A. Khan, M. A. Ellison, C. E. Schulz, W. R. Scheidt, *J. Am. Chem. Soc.* **2001**, *123*, 6314–6326; h) F. Paulat, N. Lehnert, *Inorg. Chem.* **2007**, *46*, 1547–1549.
- [6] a) P. C. Ford, L. E. Laverman, *Coord. Chem. Rev.* **2005**, *249*, 391–403; b) K. M. Miranda, X. Bu, I. Lorkovi, P. C. Ford, *Inorg. Chem.* **1997**, *36*, 4838–4848; c) D. S. Bohle, C. H. Hung, B. D. Smith, *Inorg. Chem.* **1998**, *37*, 5798–5806.
- [7] J. S. Stamler, D. J. Singel, J. Loscalzo, *Science* **1992**, *258*, 1898–1902.
- [8] a) R. García Serres, C. A. Grapperhaus, E. Bothe, E. Bill, T. Weyhermüller, F. Neese, K. Wieghardt, *J. Am. Chem. Soc.* **2004**, *126*, 5138–5153; b) P. Singh, B. Sarkar, M. Sieger, M. Niemeyer, J. Fiedler, S. Zális, W. Kaim, *Inorg. Chem.* **2006**, *45*, 4602–4609; c) M. Videla, J. S. Jacinto, R. Baggio, M. T. Garland, P. Singh, W. Kaim, L. D. Slep, J. A. Olabe, *Inorg. Chem.* **2006**, *45*, 8608–8617; d) M. Sieger, B. Sarkar, S. Zális, J. Fiedler, N. Escola, F. Doctorovich, J. A. Olabe, W. Kaim, *Dalton Trans.* **2004**, 1797–1800; e) C. M. Carter, J. Lee, C. A. Hixson, D. R. Powell, R. A. Wheeler, M. J. Shaw, G. B. Richter-Addo, *Dalton Trans.* **2006**, 1338–1346; f) Z. N. Zahran, M. J. Shaw, M. A. Khan, G. B. Richter-Addo, *Inorg. Chem.* **2006**, *45*, 2661–2668; g) P. Singh, J. Fiedler, S. Zális, C. Duboc, M. Niemeyer, F. Lissner, Th. Schleid, W. Kaim, *Inorg. Chem.* **2007**, *46*, 9254–9261; h) P. Singh, A. K. Das, B. Sarkar, M. Niemeyer, F. Roncaroli, J. A.

- Olabe, J. Fiedler, S. Zális, W. Kaim, *Inorg. Chem.* **2008**, *47*, 7106–7113.
- [9] a) J. A. McCleverty, *Chem. Rev.* **2004**, *104*, 403–418; b) G. R. A. Wyllie, W. R. Scheidt, *Chem. Rev.* **2002**, *102*, 1067–1089.
- [10] V. K. K. Praneeth, F. Paulat, T. C. Berto, S. D. George, C. Näther, C. D. Sulok, N. Lehnert, *J. Am. Chem. Soc.* **2008**, *130*, 15288–15303.
- [11] a) D. Lancon, K. M. Kadish, *J. Am. Chem. Soc.* **1983**, *105*, 5610–5617; b) L. Olson, D. Schaefer, D. Lancon, K. M. Kadish, *J. Am. Chem. Soc.* **1982**, *104*, 2042–2044; c) X. H. Mu, K. M. Kadish, *Inorg. Chem.* **1988**, *27*, 4720–4725.
- [12] Y. Liu, C. DeSilva, M. D. Ryan, *Inorg. Chim. Acta* **1997**, *258*, 247–255.
- [13] Z. Wei, M. D. Ryan, *Inorg. Chem.* **2010**, *49*, 6948–6954.
- [14] a) K. M. Kadish, Z. Ou, X. Tan, T. Boschi, D. Monti, V. Fares, P. Tagliatesta, *J. Chem. Soc. Dalton Trans.* **1999**, 1595–1601; b) A. D. Kini, J. Washington, C. P. Kubiak, B. H. Morimoto, *Inorg. Chem.* **1996**, *35*, 6904–6906; c) G. B. Richter-Addo, S. J. Hodge, G. Yi, M. A. Khan, T. Ma, E. Van Caemelbecke, N. Guo, K. M. Kadish, *Inorg. Chem.* **1996**, *35*, 6530–6538.
- [15] J. Pellegrino, S. E. Bari, D. E. Bikiel, F. Doctorovich, *J. Am. Chem. Soc.* **2010**, *132*, 989–995.
- [16] I. K. Choi, Y. Liu, D. Feng, K. J. Paeng, M. D. Ryan, *Inorg. Chem.* **1991**, *30*, 1832–1839.
- [17] M. W. Grinstaff, M. G. Hill, E. R. Birnbaum, W. P. Schaefer, J. A. Labinger, H. B. Gray, *Inorg. Chem.* **1995**, *34*, 4896–4902.
- [18] W. J. Evans, M. Fang, J. E. Bates, F. Furche, J. W. Ziller, M. D. Kiesz, J. I. Zink, *Nature Chem.* **2010**, *2*, 644–647.
- [19] N. Lehnert, V. K. K. Praneeth, F. Paulat, *J. Comput. Chem.* **2006**, *27*, 1338–1351.
- [20] A. Ghosh, P. R. Taylor, *J. Chem. Theory Comput.* **2005**, *1*, 597–600.
- [21] a) A. Ikezaki, M. Takahashi, M. Nakamura, *Angew. Chem.* **2009**, *121*, 6418–6421; *Angew. Chem. Int. Ed.* **2009**, *48*, 6300–6303; b) M. Nakamura, *Coord. Chem. Rev.* **2006**, *250*, 2271–2294.
- [22] a) S. Neya, A. Takahashi, H. Ode, T. Hoshino, A. Ikezaki, Y. Ohgo, M. Takahashi, Y. Furutani, V. A. Lorenz-Fonfria, H. Kandori, H. Hiramatsu, T. Kitagawa, J. Teraoka, N. Funasaki, M. Nakamura, *Bull. Chem. Soc., Jpn.* **2008**, *81*, 136–141; b) R. Weiss, A. Gold, J. Turner, *Chem. Rev.* **2006**, *106*, 2550–2579; c) V. Schünemann, M. Gerdan, A. X. Trautwein, N. Haoudi, D. Mandon, J. Fischer, R. Weiss, *Angew. Chem.* **1999**, *111*, 3376–3379; *Angew. Chem. Int. Ed.* **1999**, *38*, 3181–3183.
- [23] The effect of perhalogen-substituted standard ligands on the resulting coordination compounds has been described before for octachloro-1,10-phenanthroline, see: a) C. Titze, W. Kaim, *Z. Naturforsch. B* **1996**, *51*, 981–988; b) C. Titze, W. Kaim, S. Zális, *Inorg. Chem.* **1997**, *36*, 2505–2510.
- [24] a) E. R. Birnbaum, J. A. Hodge, M. W. Grinstaff, W. P. Schaefer, L. Henling, J. A. Labinger, J. E. Bercaw, H. B. Gray, *Inorg. Chem.* **1995**, *34*, 3625–3632; b) A. D. Adler, F. R. Longo, F. Kampas, J. Kim, *J. Inorg. Nucl. Chem.* **1970**, *32*, 2443–2445.
- [25] Gaussian 03, Revision C.02, M. J. Frisch, G. W. Trucks, H. B. Schlegel, G. E. Scuseria, M. A. Robb, J. R. Cheeseman, J. A. Montgomery, Jr., T. Vreven, K. N. Kudin, J. C. Burant, J. M. Millam, S. S. Iyengar, J. Tomasi, V. Barone, B. Mennucci, M. Cossi, G. Scalmani, N. Rega, G. A. Petersson, H. Nakatsuji, M. Hada, M. Ehara, K. Toyota, R. Fukuda, J. Hasegawa, M. Ishida, T. Nakajima, Y. Honda, O. Kitao, H. Nakai, M. Klene, X. Li, J. E. Knox, H. P. Hratchian, J. B. Cross, V. Bakken, C. Adamo, J. Jaramillo, R. Gomperts, R. E. Stratmann, O. Yazyev, A. J. Austin, R. Cammi, C. Pomelli, J. W. Ochterski, P. Y. Ayala, K. Morokuma, G. A. Voth, P. Salvador, J. J. Dannenberg, V. G. Zakrzewski, S. Dapprich, A. D. Daniels, M. C. Strain, O. Farkas, D. K. Malick, A. D. Rabuck, K. Raghavachari, J. B. Foresman, J. V. Ortiz, Q. Cui, A. G. Baboul, S. Clifford, J. Cioslowski, B. B. Stefanov, G. Liu, A. Liashenko, P. Piskorz, I. Komaromi, R. L. Martin, D. J. Fox, T. Keith, M. A. Al-Laham, C. Y. Peng, A. Nanayakkara, M. Challacombe, P. M. W. Gill, B. Johnson, W. Chen, M. W. Wong, C. Gonzalez, J. A. Pople, Gaussian, Inc., Wallingford CT, **2004**.

Received: December 6, 2010

Published online: May 30, 2011